Interception and rendezvous: An intuition-building approach to orbital dynamics

Eric M. Edlund

Citation: American Journal of Physics **89**, 559 (2021); doi: 10.1119/10.0003489
View online: https://doi.org/10.1119/10.0003489
View Table of Contents: https://aapt.scitation.org/toc/ajp/89/6
Published by the American Association of Physics Teachers

Interception and rendezvous: An intuition-building approach to orbital dynamics

Eric M. Edlund[a)]
Department of Physics, SUNY Cortland, Cortland, New York 13045

(Received 17 June 2020; accepted 20 January 2021)

The problem of rendezvous, the meeting of spacecraft in orbit, is an important aspect of mission planning. We imagine a situation where a chaser craft, initially traveling on the same circular orbit as its target and separated from it by a known distance, must select an initial thrust vector that will allow it to meet the target (interception) followed by a second thrust vector that will allow it to match velocities with the target (rendezvous). The analysis presented here provides solutions to this problem in simple algebraic forms while offering many rich challenges that support intuition-building exercises for students across a range of skill levels. An html-javascript orbit calculator is made available with this manuscript as a supporting visual aid and can be used to test the analysis and explore the consequences of different orbital intercept solutions.
https://doi.org/10.1119/10.0003489

I. INTRODUCTION

In his book *Carrying the Fire*, former Apollo 11 astronaut Michael Collins discusses the counter-intuitive process required for rendezvous in orbit. For example, to close a gap with a target directly ahead, pilots must slow their craft to drop into a lower altitude orbit that advances their angular position relative to the target.[1] As we will see, this maneuver is just one of many possible solutions to the interception problem. Collins describes in great detail the extensive training undertaken to make such situations second nature, including countless hours in mock-ups and simulators, the meticulous study of equipment, and the rehearsal of procedures for both planned and contingent operations. In preparation for the Apollo 11 mission, Collins trained for no less than eighteen different cases for rendezvous of the modules, since co-planar conditions could not be guaranteed. Prior to the lunar landing of Apollo 11, the Apollo 10 mission completed a lunar orbit wherein the astronauts conducted a co-planar rendezvous of the lunar module and the command and service module.

Between the earliest docking maneuvers of the Gemini and Apollo missions and the present, there have been many such feats, under diverse conditions and with a wide range of craft, both manned and unmanned. The first unmanned docking event took place in 1967 between two variants of the Soviet Soyuz spacecraft.[2] SpaceX successfully docked its Crew Dragon Module with International Space Station (ISS) twice in 2020, and the Chang'e 5 robotic probe landed on the lunar surface and returned to orbit where it docked with and transferred lunar rock samples to the orbit-return vehicle. In most of these scenarios, one of the craft (e.g., the ISS) is on an unpowered trajectory and is considered the target, while the other craft, being capable of active trajectory modification (e.g., the Crew Dragon Module), is considered the chaser. For missions to the ISS, transition onto the target's orbit for a docking maneuver typically involves initial insertion of the chaser into a holding orbit, often with a two-stage transfer through an intermediate phasing orbit, all of which is typically completed close to the orbital plane of the target.[3,4] A Hohmann transfer or bi-elliptic maneuver is often used to intercept the target. The total time for completing the rendezvous and docking of manned spacecraft with the ISS can be less than one day to as much as two days.[3]

Intermediate-level classical mechanics textbooks discuss orbital dynamics, but the mechanics of orbital intercept and rendezvous are notably absent from such discussions, which often include little more than a brief discussion of the Hohmann transfer.[5–8] Advanced, discipline-specific texts focusing on orbital dynamics often couch these discussions in the language of differential equations and three-dimensional vectors, resulting in a complete but complicated analysis that is quite challenging for undergraduate students.[4,9–11] The approach taken in this paper differs in that it avoids using differential equations[4,9,10,12–14] and instead focuses on geometric considerations.[15,16] By reducing the mathematical overhead, it emphasizes other important aspects of the general problem-solving framework, including the definition and mathematical interpretation of the intercept and rendezvous conditions, motion on elliptical orbits, the role of conserved quantities, and the utility of approximate solutions.

The central goal of this analysis is the discovery of the thrust vector for the chaser, defined in terms of a magnitude and angle that will enable it to intercept the target. Rendezvous is a second condition wherein the craft are at the same location and have matched velocities.[9] This analysis is restricted to co-orbital initial conditions that do not represent the situation of most intercept and rendezvous maneuvers, though this situation might arise, for example, when relocating craft that were placed in co-orbital trajectories for prior purposes or for practice of orbital maneuvers as was done on the Apollo 10 mission. Within these limitations, the analysis presented here seeks all possible solutions for orbital intercept given co-orbital initial conditions, including solutions of multiple and disparate number of orbits between the two craft. Simulations were and continue to be an important aspect of flight training,[1] and when used appropriately, allow the user repeated opportunities to apply theory to complete specific tasks. An auxiliary html-javascript orbit calculator accompanying this paper provides a visual aid that can be used to explore the consequences of various trajectory changes, including sensitivity to control parameters.

In Sec. II, we provide a mathematical definition of the specific problem being solved, then examine the details of the orbital characteristics of the target and chaser in Sec. III, completing the setup with a definition of the conditions required for interception in Sec. IV. We then examine a range of intercept solutions in Sec. V, consider sensitivity to control parameters in Sec. VI, analyze the rendezvous maneuver in Sec. VII, and conclude in Sec. VIII. The Appendix complements the body of the work and presents a derivation of the approximate form for the thrust magnitude used in Sec. VI.

II. DEFINITION OF THE PROBLEM

Our problem can be split into two main parts: trajectory modification by an impulsive velocity change that allows the chaser to intercept the target (the intercept problem), followed by a second impulsive maneuver that matches the velocities of the two spacecraft (the rendezvous problem). Most of the analysis is focused on the more difficult problem of intercept, which can be succinctly stated as follows: given two craft that are initially co-orbital on circular orbits and separated by a known distance, we seek the thrust vector of the impulse that will allow the chaser to intercept the target by placing the two craft at the same location at the same time. For simplicity, we assume that the change in velocity induced by the engines of the chaser occurs over a time scale so much shorter than the orbital time scales that the engine burn can be considered effectively instantaneous.

We use a fixed coordinate system with the origin at the center of force (the planetary center), as shown in Fig. 1, with the thrust vector defined in Fig. 2. Mathematical formulas will express angles in radians, whereas the figures express angles in degrees, the traditional style of navigation. In the following, the subscript "t" identifies the target variables and the subscript "c" identifies the chaser variables. Given initially co-orbital and circular orbits of the craft with initial conditions

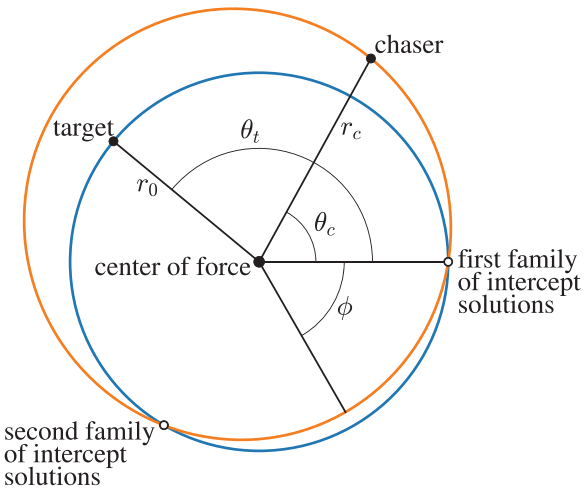

Fig. 1. Definition of the coordinate system used in this analysis, where the target remains on a circular orbit defined by radius r_0 with an angular position of θ_t, and the chaser moves on an elliptical orbit defined by radial position r_c and angular position θ_c. Note that the angular coordinates for the craft are measured in the counter-clockwise direction, whereas ϕ is measured in the clockwise direction.

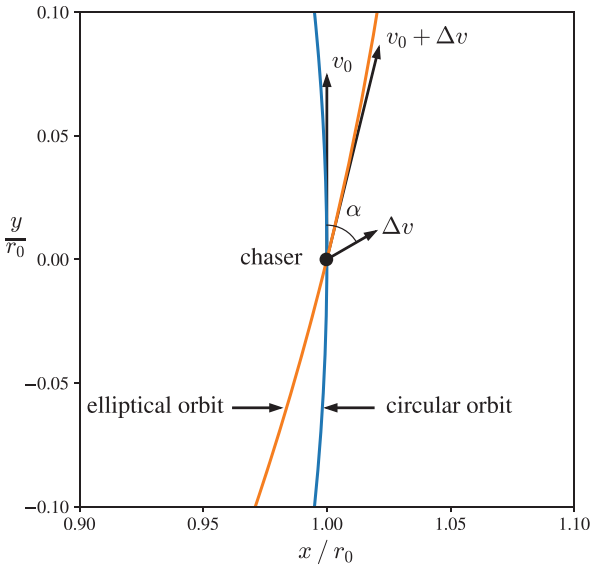

Fig. 2. Definition of the thrust vector in terms of the thrust angle α and magnitude Δv. Note that α is measured in the clockwise direction.

$$\theta_{t,i} = \theta_0, \tag{1}$$

$$\theta_{c,i} = 0, \tag{2}$$

$$r_{t,i} = r_{c,i} \equiv r_0, \tag{3}$$

where θ_0 and r_0 are known, the intercept problem presented here seeks solutions for the thrust angle α and normalized thrust magnitude $\delta = \Delta v/v_0$, where v_0 is the initial speed of the craft and Δv is the magnitude of the change in velocity, such that the following final conditions are satisfied at some unknown final time t_f:

$$\theta_{t,f} = \theta_{c,f} \quad (\text{modulo } 2\pi), \tag{4}$$

$$r_{t,f} = r_{c,f} = r_0. \tag{5}$$

The last equality in Eq. (5) follows from the fact that the target stays on a circular orbit. The rendezvous problem that concludes this analysis seeks the thrust vector that recircularizes the orbit of the chaser such that its velocity matches that of the target upon interception.

III. DESCRIPTION OF THE ORBITS

In this section, we derive expressions for the orbital period of each craft and equations for the parameters describing the elliptical trajectory of the chaser, being the orbital eccentricity ϵ, and the orbital phase angle ϕ, in terms of the control parameters α and δ. Any change in velocity of a craft on a circular orbit, except for a complete reversal of the velocity, will cause it to transition onto an elliptical orbit. While it is possible that this new elliptical orbit can have the same orbital period as the original circular orbit, in general, they are not equal. This difference in orbital period means that the elliptical orbit, when chosen correctly, serves as a phasing orbit[3,9] that allows the chaser to intercept the target.

To derive expressions for the orbital periods, we recall that Kepler's third law relates the square of the period to the cube of the semi-major axis a. The semi-major axis of the target, which remains on a circular orbit, is just the radius of

orbit r_0. To find the semi-major axis for the chaser, we first consider the shape of the chaser's elliptical orbit, which is described by

$$r_c(\theta_c) = r_0 \frac{1 + \epsilon \cos(\phi)}{1 + \epsilon \cos(\theta_c + \phi)}, \tag{6}$$

where the form of the numerator has been chosen so that $r_c(0) = r_0$, as required by the initial conditions stated in Eqs. (2) and (3). By comparing the definition of apogee, $r_{apogee} = a(1+\epsilon)$, to the maximum value of r_c in Eq. (6), $r_{max} = r_0(1+\epsilon\cos(\phi))/(1-\epsilon)$, we find $a = r_0(1+\epsilon\cos(\phi))/(1-\epsilon^2)$. Expressing Kepler's third law in terms of the ratios of quantities for the chaser and target gives $T_c/T_t = (a/r_0)^{3/2}$, or

$$T_c = T_t \left(\frac{1 + \epsilon \cos(\phi)}{1 - \epsilon^2} \right)^{3/2}. \tag{7}$$

The absolute time scale in Eq. (7) is defined by $T_t = 2\pi r_0/v_0$, where v_0 is the speed of the target on its circular orbit. It is often the case that the orbital radius is set by mission-specific considerations, such as the need to remain outside the atmosphere, energy considerations for launch, and other goals. Hence, the speed of the craft can be interpreted as a dependent quantity, whose value is determined by the radial component of Newton's second law of motion for the target, which provides the following relationship:

$$r_0 v_0^2 = GM, \tag{8}$$

where G is the universal gravitational constant, and M is the planetary mass (taken to be a spherical object that can be represented as a point mass at the origin).

We now derive the relationships between the parameters describing the geometry of the chaser's elliptical orbit and the control parameters α and δ. The azimuthal and radial velocities can be determined from the kinematics by referring to Fig. 2, where we see that the components of the chaser's velocity following engine burn are $v_{\theta,i} = v_0(1+\delta\cos(\alpha))$ and $v_{r,i} = v_0\,\delta\sin(\alpha)$. These velocities may also be expressed in terms of the dynamical variables as $v_\theta = r_c\,\dot{\theta}_c$ and $v_r = (dr_c/d\theta_c)\,\dot{\theta}_c$, where the latter is the derivative of Eq. (6) with respect to time, considering that the time dependence in that equation enters as $\theta_c = \theta_c(t)$. Equating the ratio of the dynamical velocities, evaluated at $t = 0$, to the ratio of the kinematic velocities provides

$$\left.\frac{v_r}{v_\theta}\right|_{t=0} = \left.\frac{1}{r_{c,i}}\frac{dr_c}{d\theta_c}\right|_{t=0} = \frac{\epsilon\sin(\phi)}{1+\epsilon\cos(\phi)} = \frac{\delta\sin(\alpha)}{1+\delta\cos(\alpha)}. \tag{9}$$

While it is tempting to infer from Eq. (9) that $\epsilon = \delta$ and $\phi = \alpha$, a second equation is needed to solve for the relationships between the geometric and control variables.

The total energy is a constant of the motion and must have the same value at perigee (minimum radius, maximum speed) and at apogee (maximum radius, minimum speed). Due to the presence of terms with $\pm\epsilon$ in the expressions for the radius and velocity at these points, we will identify perigee with the "+" symbol and apogee with the "–" symbol. The maximum and minimum values of r in Eq. (6) are

$$r_\pm = r_0 \frac{1 + \epsilon\cos(\phi)}{1 \pm \epsilon}. \tag{10}$$

The azimuthal velocity at these points, defined similarly as $v_\pm$, can be derived from the angular momentum. The specific angular momentum following engine burn is a constant of the motion, and can be expressed as $l_c = r_0\,v_{\theta,i} = r_0\,v_0(1+\delta\cos(\alpha))$. Equating the specific angular momentum at apogee and perigee with the initial value gives $v_\pm = l_c/r_\pm$,

$$v_\pm = v_0(1+\delta\cos(\alpha))\frac{1\pm\epsilon}{1+\epsilon\cos(\phi)}. \tag{11}$$

The radial velocity at apogee and perigee is identically zero, leading to the simple expression for the specific energy of the chaser at these points, $e = E_c/m_c = (1/2)v_\pm^2 - GM/r_\pm$. Replacing GM with $r_0 v_0^2$ (see Eq. (8)) and using the prior equations for $r_\pm$ and $v_\pm$, we have

$$e = \frac{1}{2}\frac{v_0^2}{(1+\epsilon\cos(\phi))^2}\left[(1+\delta\cos(\alpha))^2(1\pm\epsilon)^2 - 2(1\pm\epsilon)(1+\epsilon\cos(\phi))\right]. \tag{12}$$

For the total energy to be constant of the motion, the $\pm$ terms in the Eq. (12) must cancel, which yields

$$\epsilon\cos(\phi) = \delta\cos(\alpha)(2+\delta\cos(\alpha)). \tag{13}$$

We can now use the prior result together with the equality established in Eq. (9) to solve for $\epsilon\sin(\phi)$

$$\epsilon\sin(\phi) = \delta\sin(\alpha)(1+\delta\cos(\alpha)). \tag{14}$$

The ratio of Eq. (14) to Eq. (13) provides a solution for $\tan(\phi)$ in terms of the control parameters

$$\tan(\phi) = \tan(\alpha)\frac{1+\delta\cos(\alpha)}{2+\delta\cos(\alpha)}. \tag{15}$$

A solution for ϵ readily follows by squaring and summing Eqs. (13) and (14), and then taking the square root to give

$$\epsilon = \delta\sqrt{\sin^2(\alpha)(1+\delta\cos(\alpha))^2 + \cos^2(\alpha)(2+\delta\cos(\alpha))^2}. \tag{16}$$

Solutions for ϵ and ϕ as a function of α for $\delta = 0.05$, $\delta = 0.10$, and $\delta = 0.20$ are presented in Figs. 3 and 4, respectively. An interesting result of this analysis is that ϕ has very weak dependence on δ, with $\phi = \tan^{-1}(1/2\tan(\alpha))$ as $\delta \to 0$. For $\delta = 0.05$, the deviation of ϕ from this limit is everywhere less than half of a degree.

Eccentricities for near-Earth orbital-transfer maneuvers are typically in the range of a few percent for phasing orbits or Hohmann transfers between orbits.[3,4] The analysis in Sec. V begins by examining comparatively large values of ϵ to better illustrate the relationship between the period and shape of elliptical orbits, an important aspect of the intuition-building component of these studies, though the final analysis returns to a discussion of small δ, and therefore small ϵ solutions. Beyond the technical feasibility of large thrust maneuvers, it should be noted that an important

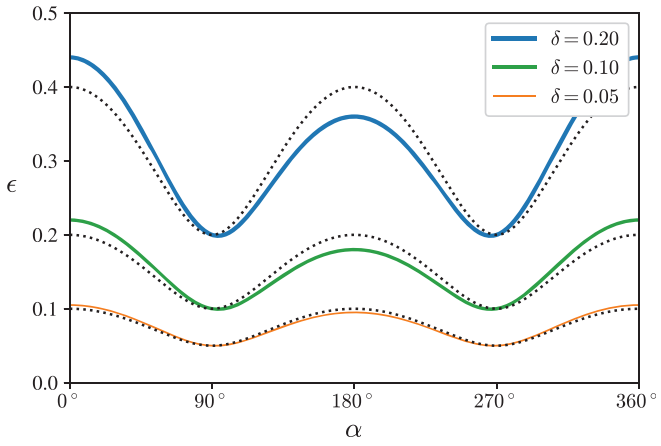

Fig. 3. The orbital eccentricity ϵ is calculated for $\delta = 0.20$ (solid thick line, top), $\delta = 0.10$ (solid medium line, middle), and $\delta = 0.05$ (solid thin line, bottom). The dotted lines are the first order (in δ) approximations for the eccentricity, that is, $\epsilon \approx \delta\sqrt{\sin^2(\alpha) + 4\cos^2(\alpha)}$. This produces an approximately 7% maximum error for the $\delta = 0.20$ case and an approximately 1.7% maximum error in the $\delta = 0.05$ case.

consequence of using a large value of thrust that slows a craft and places it into a low altitude trajectory is that the craft will at some point be slowed by the atmosphere or, worse yet, the planetary surface.

IV. TRAJECTORY INTERCEPTION

The condition that the craft have the same radial position at interception leads to two families of solutions: the starting position of the chaser ($\theta = 0$, $r = r_0$), and a second location that depends on the specifics of the chaser's elliptical orbit, as indicated in Fig. 1. While the following discussion examines only the first family of intercept conditions, it should be noted that the methods presented here can be generalized, with some additional mathematical complexity, to the second family of intercept conditions. Focusing on the first family of intercept conditions simplifies the problem, because we know that the chaser will complete an integer multiple of orbits in a time equal to an integer multiple of its orbital period, for which we have the exact solution given in Eq. (7).

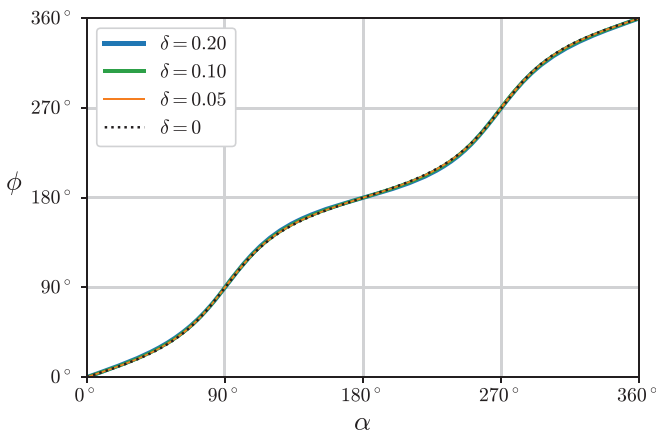

Fig. 4. The orbital rotation, ϕ, is calculated as a function of the launch angle α for $\delta = 0.20$, $\delta = 0.10$, and $\delta = 0.05$. The black dotted curve is the limiting case of $\delta = 0$. The differences between the curves are so small at this scale that they are nearly indistinguishable from each other.

To develop the intercept criterion given the constraint of interception at the initial position of the chaser, we next consider the angular coordinates of each craft. The angular coordinate of the target on its circular orbit increases linearly in time as

$$\theta_t(t) = \theta_0 + \omega_t t, \tag{17}$$

where $\omega_t = 2\pi/T_t$ is the angular velocity of the target in its circular orbit. We now evaluate Eq. (17) at a final time equal to an integer multiple of the chaser's orbital period, that is, at $t_f = n_c T_c$ where n_c counts the number of orbits of the chaser. The intercept condition follows from the requirement that the target also be at the initial position of the chaser at this final time, that is $\theta_{tf} = 2\pi n_t$, where n_t counts the number of times that the target has passed through $\theta = 0$. This gives us the intercept condition

$$2\pi n_t = \theta_0 + 2\pi n_c \left(\frac{1 + \epsilon\cos(\phi)}{1 - \epsilon^2}\right)^{3/2}. \tag{18}$$

Equation (18), together with the expressions for ϕ and ϵ in Eqs. (15) and (16), are the primary equations for this work, and will provide the main relationships for studying intercept as a function of the control parameters in the remainder of the analysis. The goal now is to find the values of α and δ that solve the intercept problem as formulated in Eq. (18).

We briefly discuss how Eq. (18) can be generalized to the second family of intercept solutions. First, we note that the symmetry of the orbit (see Fig. 1) requires that the angular position of the second orbital intersection is equal to $2\pi - 2\phi$, modulo 2π. With this information, it is possible to define the time it takes for the chaser to reach this position as an integral expression over its trajectory. This time can be found by inverting the expression for the specific angular momentum to solve for the angular velocity of the chaser, that is, $\dot{\theta}_c = l_c/r_c^2$. Separating the differentials, we have $dt = (r_c^2/l_c)\, d\theta_c$, which can be integrated to derive an expression for the intercept time, to be used in Eq. (17) in much the same way as was done for the case above. It should be noted that the integral over $d\theta_c$ requires numerical integration or a suitable approximation, since r_c is a function of θ_c, and is further complicated by the fact that the upper limit of this integral is a function of the intercept angle.

V. INTERCEPT SOLUTIONS

Any value of δ will enable intercept solutions if the crew of the chaser is able to wait long enough. The following analysis will consider two approaches to our study of intercept solutions: a case with a large value of δ as an illustrative example of the solution space, followed by comparison of solutions for different values of δ.

As a first case, we consider $\theta_0 = 15°$ and search for the values of α that provide interception within three orbits of the target, by considering a large thrust maneuver with $\delta = 0.20$. Graphical representations of Eq. (18) are presented in Fig. 5, where the LHS of this equation is represented by the horizontal lines, and the RHS by the colored curves (online only). An intercept solution exists at each crossing of a curve with a horizontal line. Under the conditions considered here, there are 12 values of α that will enable interception within three orbits of the target. Figure 6 shows the trajectories of both craft for the $\alpha = 260.1°$ solution,

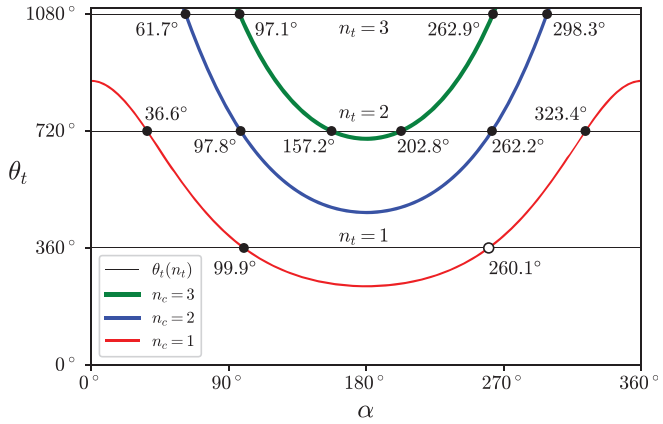

Fig. 5. Solution space for the conditions $\theta_0 = 15°$ and $\delta = 0.20$. The open marker for $\alpha = 260.1°$ identifies the solution corresponding to the trajectory plot presented in Fig. 6.

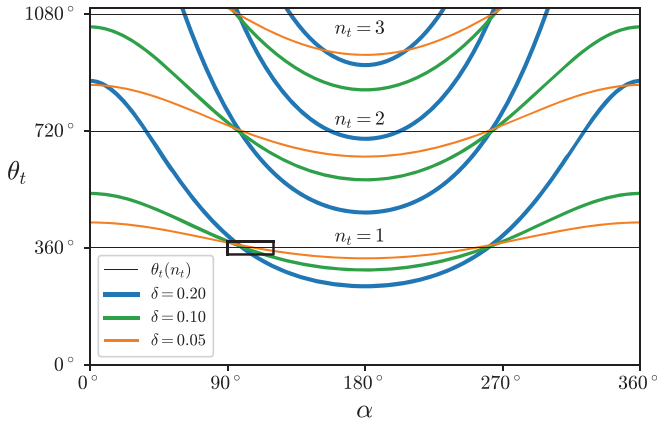

Fig. 7. Comparison of solution curves for Eq. (18) for different values of δ. The black box near $\alpha = 90°$ defines the plot region of Fig. 8.

illustrating how the chaser initially moves onto a lower altitude trajectory and moves ahead of the target, and then onto a higher altitude trajectory where its angular velocity slows, allowing the target to catch up to it, arriving at the chaser's initial location simultaneously with the target.

A second perspective on this problem examines the allowable combinations of δ and α when n_t, n_c, and θ_0 are prescribed, effectively defining the time to interception. This is a more challenging analysis, largely on account of the complicated relationship between δ and α that arises when Eq. (18) is presented in terms of these variables. While it is possible, in principle, to perform an algebraic inversion of Eq. (18) to solve for δ as a function of α, the equation that emerges is fourth order in δ and does not readily lead to new insights. Instead, we consider the approach of a parameter scan in δ and examine the patterns that emerge.

Figure 7 presents the graphical solutions to Eq. (18), similar to Fig. 5, but with multiple curves corresponding to different values of δ. First, we note that of the three values of δ presented, only the $\delta = 0.20$ solutions are able to produce solutions with disparate numbers of orbits for $n_t \leq 3$. We also note that the majority of solutions tend to fall between 90° and 270°, indicating thrust vectors that slow the chaser. This should be expected since thrusts with a substantial backward component[17] will reduce the chaser's period, allowing it to catch up with a target that has a small, positive initial angular separation. Another interesting pattern that emerges is that clusters of solutions occur in the neighborhoods of 90° and 270° for different values of δ. While at first this may seem like a good quality since multiple intercept solutions are accessible, on further consideration it reveals exactly the opposite: orbital intercept using a value of α near 90° or 270° will exhibit large sensitivity to the thrust angle. That is, small deviations from the ideal thrust angle will require substantial changes in δ to ensure interception. Therefore, these points are less desirable from the perspective of control systems, where we would prefer to have low sensitivity to the thrust parameters. Section VI investigates the issue of sensitivity to errors in the control parameters in greater depth.

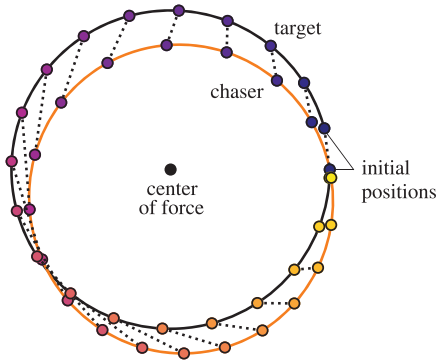

Fig. 6. Strobe-effect plot of the orbital positions of the target and chaser, corresponding to the $\alpha = 260.1°$ solution from Fig. 5, where the markers indicate the position of each craft at constant intervals in time, proceeding from dark to light. The dashed lines between the markers identify position pairs of the target and chaser for each time point.

VI. SENSITIVITY TO VARIATIONS IN THE CONTROL PARAMETERS

A full analysis of system sensitivities is an interesting subject, but necessarily involves additional mathematical treatment and discussion regarding the definition of small or tolerable variations, which places this subject beyond the scope of this work. Instead, we motivate a simplified picture of sensitivity through the question: what combinations of thrust angle and thrust magnitude make for a particularly robust intercept solution when considering small errors in α? The answer is that low sensitivity is equivalent to the

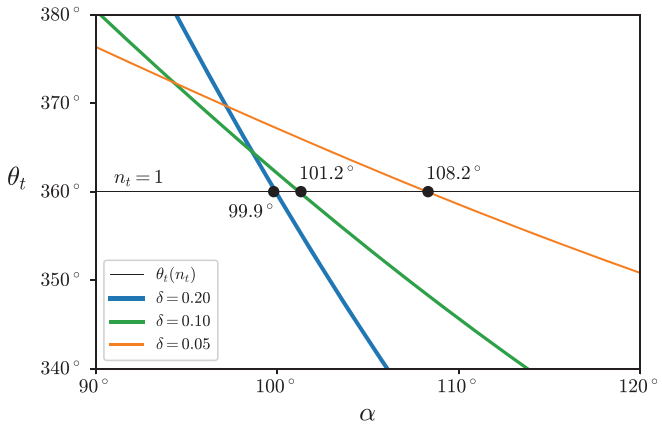

Fig. 8. Zoomed-in view of the intercept solutions in the vicinity of $\alpha = 90°$ for $n_t = 1$ for the three different values of δ presented in Fig. 7.

statement that a curve of Fig. 7 has a small slope in the neighborhood of a solution. This can be understood by returning to the meaning of the curves, which is the angular position of the target when the chaser has returned to its starting position, as described in Eq. (18). Therefore, the effect of a small deviation in α from the ideal intercept value can be visualized as movement along the curve, with the vertical distance between the value of θ_t and the intercept value being the angular separation between the target and chaser. It follows that curves with a small slope near the intercept solution imply that the position of the target will not vary greatly as a function of α. For example, Fig. 8 shows that the $\delta = 0.05$ curve has substantially lower slope than the $\delta = 0.20$ curve in the vicinity of $\alpha = 90°$, and will therefore exhibit smaller variation in the difference of the angular positions of the target and chaser, a hypothesis that can be readily tested with the orbit calculator.

Optimal robustness against variations in α will occur where the slope of the curve is zero at intercept, requiring that it be tangent to one of the horizontal lines. Referring back to Fig. 5, we observe that the $\delta = 0.20$ curve has lower slope for the $n_t = 2$, $n_c = 3$ solutions (compared to its other solutions), and it seems reasonable to guess that a value of δ slightly less than 0.20 will be tangent to the $n_t = 2$ line and provide an optimally insensitive solution with respect to variations in α. In the following, we examine the specific conditions required for optimal insensitivity to deviations in α from the ideal values.

The lowest sensitivity solutions require $\alpha = 0°$ or $\alpha = 180°$, an unsurprising result.[18] Restricting our search to these values, noting that $\cos(\alpha) = \pm 1$, and rearranging Eq. (18) we have

$$\left[\frac{2\pi n_t - \theta_0}{2\pi n_c}\right]^{2/3} = \frac{1 \pm \epsilon}{1 - \epsilon^2} = \frac{1}{1 \mp \epsilon} = \frac{1}{1 \mp \delta(2 \pm \delta)}, \tag{19}$$

where the last equality comes from using $\epsilon = \delta(2 \pm \delta)$, the form of Eq. (16) under $\alpha = 0°$ or $\alpha = 180°$, respectively. Equation (19) is quadratic in δ, and further details of its solution and subsequent approximations can be found in the Appendix. Defining the LHS of Eq. (19) as f, we find the following two solutions for δ:

$$\delta_\pm = \pm\left(\sqrt{2 - \frac{1}{f}} - 1\right), \tag{20}$$

where the $+$ solution corresponds to $\alpha = 0°$ and the $-$ solution to $\alpha = 180°$. Noting that the solutions for δ_+ and δ_- have the same magnitude, only one of them can be realized for a given set of orbital n_t and n_c, that is, for a given value of f. Which one of these solutions is feasible (i.e., positive) depends on whether the value of f is greater than or less than unity, respectively. Returning to the example noted in the earlier discussion of Fig. 5, if $n_t = 2$, $n_c = 3$, and $\theta_0 = 15°$, then $f \approx 0.753$ and we calculate an optimal solution of $\delta_- \approx 0.181$ with $\alpha = 180°$, in agreement with the guess posited earlier that a value slightly less than $\delta = 0.20$ would be necessary to achieve an interception that is optimally insensitive to variations in α.

Finally, we use the results of the preceding analysis to find optimally insensitive solutions for small values of δ that are more realistic of current technology and near-Earth orbits. Low-energy intercept maneuvers allow the chaser to slowly gain position on the target, closing the gap over multiple orbits. This is equivalent to the statement that these low-energy maneuvers require $n_c = n_t$. Under these conditions, and when the initial angle of separation is small, a Taylor series expansion for f becomes feasible. Following a series of approximations, presented in full detail in the Appendix, we find $\delta_- \approx \theta_0/6\pi n_t$, or when θ is measured in degrees $\delta_- \approx \theta_0/1080° n_t$. For the cases explored earlier where $\theta_0 = 15°$, we find $\delta_- \approx 0.0139$ for $n_t = 1$, and $\delta_- \approx 0.00278$ for $n_t = 5$. These values should be contrasted with the exact values (to three digits of significance) derived from Eq. (20) of 0.0145 and 0.00280, showing errors of approximately 4% and 0.7%, respectively. The orbit simulator provided with this manuscript can be used to test these calculations and explore the concept of sensitivity by, for example, varying the thrust angle within a specific error range and examining the effect on the final positions of the target and chaser for different values of δ.

VII. RENDEZVOUS

With the solutions for the thrust angles that allow the chaser to intercept the target now in hand, the only remaining part of the analysis is to determine what second thrust maneuver is required to match the velocity of the chaser with that of the target upon interception. Under the conditions examined here, intercept occurs at the initial position of the chaser (i.e., $\theta = 0$). Because the chaser travels on an elliptical orbit, it follows that the chaser will have the same velocity whenever it passes through the initial point. In order to allow the chaser to match velocity with the target at that moment, a thrust vector equal and opposite to that initially provided for the intercept maneuver is necessary to recircularize the orbit. It may seem disturbing that the rendezvous maneuver for a chaser that began an intercept maneuver with a reverse thrust ($\alpha = 180°$), for example, will require the pilot to apply a forward thrust aimed directly at the target at a moment when the two craft are already very close. It is not surprising that nerves of steel are required in piloting spacecraft that seem to do the opposite of what our intuition tells us is correct, a fact well described by Michael Collins and other astronauts.

VIII. CONCLUSIONS

A number of entertaining and challenging puzzles emerge from consideration of intercept and rendezvous maneuvers, and there are many parts of this story that have been left untouched in this analysis, such as the second family of possible intercept solutions that requires a more complicated mathematical treatment. While conceptually simple, even the reduced interception problem presented here is difficult because it is an inherently three dimensional intersection problem, requiring co-location in the radial and angular coordinates, and simultaneous arrival. The goal of the reduction in complexity of the analysis presented here is to help build physical intuition of the temporal evolution of motion on elliptical orbits that is central to interception problem.

One of the main results of this work, naturally emerging from the method of graphical solution, is the interpretation of orbits in terms of sensitivity to control parameters. We noticed that curves with small derivative with respect to α tend to be rather insensitive to small errors in α. In contrast,

the confluence of curves with different values of δ in the neighborhoods of $\alpha = 90^\circ$ and $\alpha = 270^\circ$, where the slopes are comparatively large, indicates that these are unlikely candidates for actual intercept and rendezvous missions given the extreme sensitivity to α, despite being valid mathematical solutions to the intercept problem.

The orbit calculator tool provided with this manuscript allows users to experience the problem from the perspective of a pilot on board the chaser craft who is in charge of selecting the thrust angle and magnitude to complete the intercept maneuver.[19] This calculator provides a method for checking answers derived from the analysis, such as the remarkably simple solution of $\delta_\pm \approx \mp\theta_0/6\pi n_t$ for forward (+) or reverse (–) thrusts. It also allows users to observe the consequences of various solutions and demonstrates the importance of sensitivity studies. For example, it becomes quickly apparent that one of the great benefits to using a small δ maneuver that takes multiple passes, as compared to a large δ maneuver that completes interception in few orbits, is that the potential for error arising in miscalculation or misapplication of α or δ is greatly diminished by dividing that error over multiple passes that allows the pilot time to make small corrections to fine-tune the chaser's intercept trajectory.

ACKNOWLEDGMENTS

The author would like to thank the students from his Classical Mechanics course who asked many great questions in the discussions of the interception and rendezvous problems, and were the inspiration to transform those lectures into this written work. The author would also like to give special thanks to Professor Jonathan Levine who discovered an error in the first version of this work and generously provided a detailed analysis of the problem, and also provided many useful suggestions for improving this manuscript.

APPENDIX: DERIVATION OF THE EXACT AND APPROXIMATE FORMS OF δ WHEN f IS SPECIFIED

This appendix provides a detailed analysis of the solutions for the optimal values of δ at thrust angles of $\alpha = 0^\circ$ and $\alpha = 180^\circ$. Beginning with Eq. (18),

$$2\pi n_t = \theta_0 + 2\pi n_c\left(\frac{1+\epsilon\cos(\phi)}{1-\epsilon^2}\right)^{3/2}, \tag{A1}$$

we reformulate it as

$$\left[\frac{2\pi n_t - \theta_0}{2\pi n_c}\right]^{2/3} = \frac{1+\epsilon\cos(\phi)}{1-\epsilon^2}. \tag{A2}$$

To simplify the following analysis, where we seek a solution for the thrust magnitude which enters through ϵ, we define the LHS of Eq. (A2) as $f = f(n_t, n_c, \theta_0)$. For the special cases of $\alpha = 0^\circ$ and $\alpha = 180^\circ$, the orbital eccentricity of the chaser is

$$\epsilon_\pm = \delta(2 \pm \delta), \tag{A3}$$

where the ϵ_+ solution corresponds to $\alpha = 0^\circ$ and the ϵ_- solution to $\alpha = 180^\circ$. As an aside, we note that bound orbits require $\epsilon < 1$, and this form for ϵ shows us that the chaser will escape (i.e., become unbound) for $\delta \geq \sqrt{2} - 1 \approx 0.41$ for the forward thrust case, a well-known result in orbital analysis. With these constraints, Eq. (A2) becomes

$$f = \frac{1 \pm \epsilon_\pm}{1 - \epsilon_\pm^2} = \frac{1}{1 \mp \epsilon_\pm} = \frac{1}{1 \mp \delta(2 \pm \delta)}. \tag{A4}$$

When values for n_t, n_c, and θ_0 are specified, f is defined and we can represent Eq. (A4) as a quadratic expression in δ, that is,

$$\delta^2 \pm 2\delta + \left(\frac{1}{f} - 1\right) = 0. \tag{A5}$$

Considering separate solutions for δ for the + and – cases in Eq. (A5) separately, and calling these δ_+ and δ_-, we find a total of four possible solutions for δ

$$\delta_+ = -1 \pm \sqrt{2 - \frac{1}{f}}, \tag{A6}$$

$$\delta_- = 1 \pm \sqrt{2 - \frac{1}{f}}. \tag{A7}$$

All solutions for δ must be positive, meaning that we have to dismiss the – solution in Eq. (A6). While physically possible, the + solution in Eq. (A7) is greater than unity, indicating that the chaser craft would fully change its direction of rotation, an impractical maneuver that would be both energetically and economically costly and will not be considered further. After removing these solutions, we find that the remaining two solutions have the same magnitude, hence we have

$$\delta_\pm = \pm\left(\sqrt{2 - \frac{1}{f}} - 1\right). \tag{A8}$$

A special case set of solutions arises when we require $n_c = n_t > 1$, meaning that the gap between the chaser and target is closed over multiple orbits in an efficient progression toward interception. Under these conditions, we can simplify our expression for f as

$$f(n_t, n_c, \theta_0) = (1 - \frac{\theta_0}{2\pi n_t})^{2/3}. \tag{A9}$$

When the initial angular separation between the craft is small or the number of orbits is large such that $\theta_0 \ll 2\pi n_t$, we can further simply the expression for f using a first order Taylor series approximation

$$f \approx 1 - \frac{\theta_0}{3\pi n_t}. \tag{A10}$$

Using this approximation for f in Eq. (A8), we have

$$\delta_{\pm} \approx \pm\left(\sqrt{2-\frac{1}{1-\frac{\theta_0}{3\pi n_t}}}-1\right),$$
$$\approx \pm\left(\sqrt{2-\left(1+\frac{\theta_0}{3\pi n_t}\right)}-1\right),$$
$$\approx \mp\frac{\theta_0}{6\pi n_t}, \tag{A11}$$

where in the above steps we have used two additional first-order Taylor series approximations to first simplify the fraction inside the root and then to eliminate the square root. The final form indicates that when θ_0 is positive, as was the case in the scenarios examined in this study and described by Collins,[1] we must choose the δ_- solution, which is a thrust opposite to the direction of motion. Conversely, if θ_0 is negative (chaser leading the target) we would use the δ_+ solution, indicating a forward thrust that places the chaser on a higher altitude orbit that increases its orbital period and allows the target to catch up to it.

[a]Electronic mail: eric.edlund@cortland.edu; Permanent address: PO Box 2000, Cortland 13045, New York.

[1]M. Collins, *Carrying the Fire* (Farrar, Strauss and Giroux, New York, 2009).
[2]NASA. 50 years ago: The first automatic docking in space, 2017. <https://www.nasa.gov/feature/50-years-ago-the-first-automatic-docking-in-space>.
[3]R. Murtazin, "Short profile for the human spacecraft Soyuz-TMA rendezvous mission to the ISS," Acta Astronautica **77**, 77–82 (2012).
[4]H. D. Curtis, *Orbital Mechanics for Engineering Students* (Elsevier, Amsterdam, 2014).
[5]J. B. Marion and S. T. Thornton, *Classical Dynamics* (Harcourt College Publishers, Texas, 1995).
[6]G. R. Fowles and G. L. Cassiday, *Analytical Mechanics* (Brooks Cole, California, 2005).
[7]J. R. Taylor, *Classical Mechanics* (University Science Books, California, 2005).
[8]D. R. Morin, *Introduction to Classical Mechanics* (Cambridge U. P., Cambridge, 2008).
[9]J. E. Prussing and B. A. Conway, *Orbital Mechanics* (Oxford U. P., Oxford, 2012).
[10]B. W. Carroll, "The delicate dance of orbital rendezvous," Am. J. Phys. **87**(8), 627–637 (2019).
[11]J. C. van der Ha, "Exact analytical formulation of planar relative motion," Acta Astronautica **7**(1), 1–17 (1980).
[12]R. A. Freedman, I. Helmy, and P. D. Zimmerman, "Simplified navigation for self-propelled astronauts," Am. J. Phys. **43**, 438–440 (1975).
[13]E. I. Butikov, "Relative motion of orbiting bodies," Am. J. Phys. **69**(63), 63–67 (2001).
[14]B. D. Mills, "Satellite paradox," Am. J. Phys. **27**, 115–117 (1959).
[15]D. Longcope, "Using Kepler's laws and Rutherford scattering to chart the seven gravity assists in the epic sunward journey of the Parker Solar Probe," Am. J. Phys. **88**(11), 11–19 (2020).
[16]J. C. Amato, "Flying in formation: the orbital dynamics of LISA's three spacecraft," Am. J. Phys. **87**(18), 18–23 (2019).
[17]Due to the complicated dependence of the orbital period on α and δ, through ϕ and ϵ, it is possible for thrust vectors with small backward components to increase the orbital period of the elliptical trajectory. This can be proved by evaluating the orbital period of Eq. (7) at $\alpha = \pi/2$, which results in $\phi = \pi/2$ for all values of δ, and therefore $T_c/T_t = 1/(1-\epsilon^2) > 1$. It follows that this ratio of orbital periods will continue to be greater than unity for some window of thrust vector angles greater than $\pi/2$.
[18]This can be proven by considering the derivative of the RHS of Eq. (18) with respect to α. Noting that the expression for the orbital period of the chaser depends on ϕ only through powers of $\cos(\alpha)$ after replacing the $\sin^2(\alpha)$ term with $1 - \cos^2(\alpha)$ in the expression for ϵ^2, it follows that this derivative is proportional to $\sin(\alpha)$. Therefore, $\alpha = 0°$ and $\alpha = 180°$ provide solutions with the lowest sensitivity to small deviations in α. Further analysis of this derivative shows that these are the only two possibilities.
[19]See supplementary material at https://www.scitation.org/doi/suppl/10.1119/10.0003489 for the html-javascript orbit calculator.

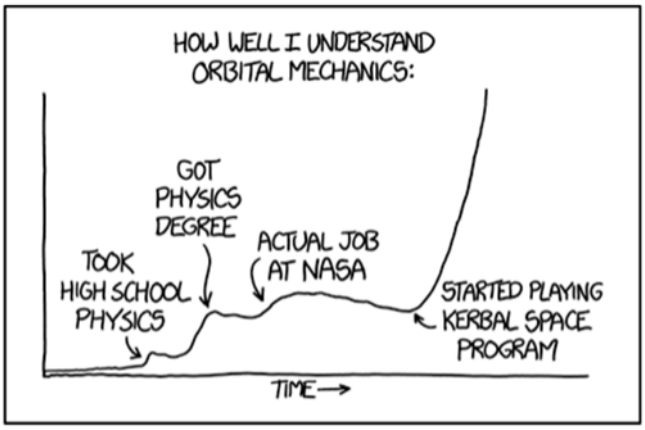

Orbital Mechanics

To be fair, my job at NASA was working on robots, and didn't actually involve any orbital mechanics. The small positive slope over that period is because it turns out that if you hang around at NASA, you get in a lot of conversations about space.
(Source: https://m.xkcd.com/1356/)